Research Article | Vol. 30, No. 19 / 12 Sep 2022 / Optics Express 33627
Optics EXPRESS

Electrically switchable capabilities of conductive polymers-based plasmonic nanodisk arrays

RUI LI,[1] XINRAN WEI,[2,3] YUZHANG LIANG,[2,3,*] HUIXUAN GAO,[2] SVETLANA KURILKINA,[4,5] AND WEI PENG[2,3]

[1]School of Optoelectronic Engineering and Instrumentation Science, Dalian University of Technology, Dalian 116024, China
[2]School of Physics, Dalian University of Technology, Dalian 116024, China
[3]DUT-BSU Joint Institute, Dalian University of Technology, Dalian 116024, China
[4]DUT-BSU Joint Institute, Dalian University of Technology, Minsk 220030, Belarus
[5]B.I.Stepanov Institute of Physics, National Academy of Sciences of Belarus, Minsk 220072, Belarus
*yzliang@dlut.edu.cn

Abstract: The electrically dynamic regulation of plasmonic nanostructures provides a promising technology for integrated and miniaturized electro-optical devices. In this work, we systematically investigate the electrical regulation of optical properties of plasmonic Au nanodisk (AuND) arrays integrated with different conductive polymers, polypyrrole (PPy), polyaniline (PANI), and poly(3,4-ethylenedioxythiophene) (PEDOT), which show their respective superiority of electrical modulation by applying the appropriate low voltages. For the hybrid structure of polymer-coated AuND arrays, its reflection spectrum and corresponding structural color are dynamically modulated by altering the complex dielectric function of the covering nanometer-thick conductive polymers based on the electrically controlled redox reaction. Due to the distinct refractive index responses of different polymers on the external voltage, polymer-coated AuND arrays exhibit different spectral variations, response time, and cycle stability. As a result, the reflection intensity of PPy-coated AuND arrays is mainly tailored by increasing optical absorption of the PPy polymer over a broad spectral range, which is distinguished from the wavelength shift of the resonance modes of AuND arrays induced by the other two polymers. Additionally, AuND arrays integrated with both PANI and PEDOT polymers exhibit a rapid switching time of less than 50 ms, which is 5 times smaller than the case of the PPy polymer. Most importantly, PPy-coated AuND arrays exhibit excellent cycle stability over 50 cycles compared to the other two polymers integrated devices. This work demonstrates a valuable technique strategy to realize high-performance polymer-coated dynamically tunable nanoscale electro-optical devices, which has especially significance for smart windows or dynamic display applications.

1. Introduction

Dynamically nanostructured electro-optical components have attracted much interest in a wide variety of applications, such as integrated optical circuits [1], high-resolution structural color generation [2,3], high-sensitivity biosensors [4], etc. It is highly desired for dynamically switchable devices with a broad spectral tunable range, short switching times, low power consumption, and long-term stability. However, substantial shortcomings hamper their development in practical application. Fortunately, the plasmonic nanostructure is a promising candidate for overcoming these limitations due to its highly confined near-field enhancement substantially increasing the interaction of light with the matter on the nanoscale [5]. Up to now, a number of plasmonic-coated dynamic nanostructure devices have been proposed by utilizing diverse mechanisms. These dynamically switchable methods are mainly summarized as two categories: one is to change

#471524 https://doi.org/10.1364/OE.471524
Journal © 2022 Received 26 Jul 2022; revised 18 Aug 2022; accepted 19 Aug 2022; published 29 Aug 2022

Optics EXPRESS

the geometry size and dielectric properties of the nanostructure itself, e. g. electrochemical deposition of metals [6], metal phase transition materials such as tungsten trioxide (WO_3) [7], titanium oxide (TiO_2) [8], magnesium (Mg) [9] and vanadium dioxide (VO_2) [10]. The other is to directly alter the refractive index response of surrounding functional materials, e.g. liquid crystals [11] and electrochemical (EC) polymers [12,13]. The abovementioned two switchable schemes are accomplished by an external stimulus, such as electrical fields, gases, ions, etc. Among these modulation approaches, integrating EC polymer on the plasmonic nanostructure is being extensively investigated for display applications due to their unique characteristics of flexible, low power consumption, low-cost and relatively simple manufacturing, and abundant selection of materials, e.g. polypyrrole, polythiophene, polyaniline, etc [14,15]. The EC polymer-coated plasmonic dynamic device is reversibly modulated by the electrically controlled redox reaction of the conductive EC polymer, where its complex dielectric function has strong variations. Notably, an ultra-thin polymer layer (less than 100 nm) is only required to achieve both a high modulation contrast and a broad regulation range by taking most of the highly confined near-field of the plasmonic nanostructure, which significantly both reduces the switching time and lowers the switching voltage. The utilization of the abovementioned high efficient EC polymer overcomes these limitations of longer switching time and severe deterioration in use due to high voltages for traditional individual EC polymer devices. Various ensembles of plasmonic nanostructures and EC polymers are taken to improve the performance of full-color switchable devices to satisfy the requirement of commercial display applications, e. g. electronic paper [16]. However, most studies to date mainly concentrate on the electrically switchable responses of the individual conductive polymer on plasmonic nanostructures. There have been a few reports on electrical regulation of the same nanostructure using different conductive polymers to compare and demonstrate the unique advantage of each polymer to realize dynamic tunable optical devices.

In this work, we experimentally demonstrate the electric modulation of the optical properties of plasmonic AuND arrays by using three ultra-thin common conductive EC polymers, PPy, PANI, and PEDOT driven by their respective reduction-to-oxidation transition. These three polymers exhibit distinct modulated properties due to different refractive index variations with externally applied voltages, resulting in different spectral superimposed responses in the hybrid structure of polymer-coated AuND arrays. The active modulation of three polymers is systematically investigated and compared in terms of reflection spectra, the corresponding color variation, switching time, and switching cycle. As a result, the ultra-thin coatings of the PPy polymer on the AuND arrays can tune its reflection intensity over a broad spectral range by simultaneously changing the real and imaginary parts of the refractive index of the polymer. As a comparison, PANI and PEDOT polymers are prone to modulate the plasmonic resonant wavelength of AuND arrays by changing their real part of the refractive index. Furthermore, both PANI and PEDOT polymers exhibit a fast switching time of less than 50 ms compared to the PPy polymer case, especially for the PEDOT polymer. However, the cycling stability is justly opposite. The PPy polymer is better, resulting in an excellent device lifetime. This research will have significant implications for the selection of conductive polymers to realize high-performance dynamic electro-optical devices.

2. Experimental procedures and apparatus

Figure 1 demonstrates the working principle of the proposed electrically switchable plasmonic device at the applied voltages of −0.5 V and 0.5 V, along with its experimental fabrication process and corresponding optical measurement setup. As shown in Fig. 1(a), the proposed electrically switchable plasmonic hybrid system is composed of centimeter-scale AuND arrays fabricated on an opaque Au membrane supported by an ITO-coated glass slide and a conformably coated thin layer of the EC polymer, the optical reflection spectrum of which can be electrically switched through the applied voltage. The mechanism of this electrical modulation is explained

Optics EXPRESS

as follows: when an external voltage is applied, electrons in the metal and ions in the electrolyte are driven to flow in (negative voltage) or out (positive voltage) of the polymer, resulting in a change of its configuration, and a concurrent variation of the complex dielectric function. The plasmonic mode of AuND arrays is highly sensitive to the external environment change within its nanometric decay length. Therefore, the effective modulation of the plasmonic mode of AuND arrays can be realized using an ultrathin EC polymer with a fast switching time due to the short charge-propagation distance. Figure 1(b) illustrates the fabrication processing of the polymer-coated AuND arrays. The specific fabrication steps are summarized as follows: firstly, a 5-nm-thick Cr adhesion layer and a 200-nm-thick opaque Au membrane are successively deposited on an ITO-coated glass slide using the magnetron sputtering equipment as a substrate. Then, a 300-nm-thick quasi-ordered porous aluminum oxide (AAO) membrane is transferred onto the fabricated substrate using the acetone solution [17]. Afterward, a 50-nm-thick gold film is deposited again onto the AAO-coated substrate. Next, the AAO membrane is peeled off by epoxy adhesive tape to form large-scale AuND arrays with a periodicity of roughly 450 nm and a 50 nm height. Notably, the diameter of AuND is random in the range from 260 nm to 360 nm. Finally, a thin layer of the conductive EC polymer is polymerized on the surface of AuND arrays in the electrolyte solution containing a certain amount of the monomer (The detailed description refers to the method section). The synthesis of three conductive EC polymers on AuND arrays and corresponding spectro-electrochemical measurements are performed in a custom-built quartz cell consisting of three electrodes, as shown in Fig. 1(c), where the AuND arrays are served as a working electrode (green filled circle dot), along with a platinum (Pt) counter electrode (red filled circle dot) and an Ag/AgCl reference electrode (white filled circle dot). The real-time optical spectrum measurement is conducted using a custom-built setup, where a broadband halogen lamp (HL-2000, Ocean Optics) and a fiber-optic spectrometer (AvaSpec-Mini4096CL) are connected to two branch ends of a bifurcated optical fiber jumper, and its common end is connected to an optical fiber collimator. The samples are irradiated with the broadband light from the collimator and the reflection light is collected using the same collimator. Combining optical spectrometer

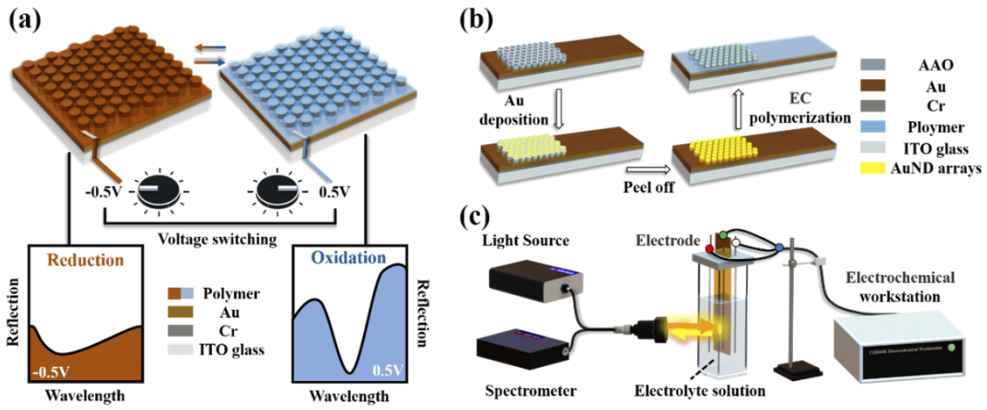

Fig. 1. The schematic of the electrically switchable EC polymer-coated plasmonic device and its experimental fabrication process and the corresponding optical measurement setup. (a) The electrical switching of conductive polymer-coated AuND arrays between the reduced (applied voltage of −0.5 V) and oxidized forms (applied voltage of +0.5 V). (b) Fabrication steps of polymer-coated AuND arrays on an opaque Au membrane supported by an ITO-coated glass slide. (c) The schematic of the electrochemical cell (three-electrode setup) and the optical measurement setup. Both the electrical polymerization of all conductive polymers on AuND arrays and the electrically switchable in-situ optical measurement are performed using the same experimental setup.

Optics EXPRESS

measurement setup with an electrochemical workstation, electrically switchable responses of various polymers-coated AuND arrays are investigated by applying various voltages.

3. Results and discussion

3.1. Electrically switchable responses of PPy-coated AuND arrays

The electrically controllable PPy polymer on plasmonic AuND arrays is first investigated due to its excellent properties of better stability, ease of electrochemical polymerization, and strong electrical conductivity [18,19]. As illustrated in Fig. 2, we investigate the optical responses of PPy-coated AuND arrays by applying low external voltages. The molecular structures of PPy in the reduced and oxidized forms are demonstrated in Fig. 2(a). Typically, neutral PPy (reduced state) can dope the anions in the electrolyte, which results in PPy with positive charges (oxidized state). The oxidized PPy maintains the charge balance with anions. Meanwhile, the anions are dedoped after the oxidized PPy gains electrons so that the PPy returns to a reduced state. To switch the optical response of AuND arrays, a thin PPy layer is electrically polymerized on the AuND arrays with cyclic voltammetry (CV) by sweeping the voltage from −0.8 V to 0.7 V versus Ag/AgCl in a solution containing $NaClO_4$ and monomer Py. Figure 2(b) demonstrates the reflection spectra of AuND arrays before and after the deposition of PPy, plotted using black and orange solid lines, respectively. Their corresponding scanning electron microscopy (SEM) images are shown in the left panel of Fig. 2(b). Obviously, the deposition of PPy polymer greatly reduces the reflection intensity of AuND arrays over a broad spectrum range from 400 nm to 900 nm due to its strong absorption characteristics in the oxidized state. To demonstrate the real-time modulated capability, the reflection spectra of PPy-coated AuND arrays immersed in a free-monomer electrolyte solution are adjusted by different voltages from −0.8 V to 0.1 V with a step of 0.05 V in Fig. 2(c). We can see that, in the fully reduced state (−0.8 V), the plasmon mode of PPy-coated AuND arrays appearing at 720 nm has a large redshift compared to the plasmon mode of naked AuND arrays at 641 nm marked by a filled orange dot in Fig. 2(b). When the applied voltage is increased, the complex dielectric function of the PPy polymer is gradually changed until the PPy reaches its fully oxidized state, resulting in a continuous decrease of reflection intensity in the wavelength range from 500 nm to 900 nm, corresponding to the absorption increase, especially for the near-infrared region around 900 nm [20].

To elucidate the origins of strong absorption induced by PPy polymer, Fig. 2(d) calculates the reflection spectra of bare AuND arrays and the structure covered by PPy in the fully reduced (−0.8 V) and oxidized (0.1 V) states. We can see clearly that the simulated results are nearly consistent with the counterpart of experimental results in terms of spectral variation tendency. Their difference mainly stems from the different geometric sizes of AuND arrays, surface roughness, and materials parameters. Notably, in the simulation, the refractive index of PPy in the fully reduced states is obtained using an Ellipsometer, as shown in Supplement 1, Fig. S1. The refractive index used in the oxidized states is two times larger than the case in the fully reduced state. Therefore, we deduce that the increase of absorption of the PPy polymer by applying the voltage from −0.8 V to 0.1 V can be attributed to the simultaneous increase of the real and imaginary parts of the refractive index of polymer from the reduced to oxidized state. Additionally, Fig. 2(e) shows the spatial electric field distributions of bare AuND arrays and AuND arrays coated by two different states of PPy layers at the wavelength of 900 nm. Compared to bare AuND arrays, strong electric field enhancement is mainly confined inside and around the dielectric layer, especially for the thin PPy in the oxidized state with a large imaginary part of the refractive index, causing low reflection intensity and concurrently high absorption.

Due to the different absorption of thin PPy polymer under varied voltages, the color of PPy-coated AuND arrays can be dynamically fine-tuned by changing the applied voltages. Figure 3(a) demonstrates the calculated color palettes of PPy-coated AuND arrays at the voltages from −0.8 V

Optics EXPRESS

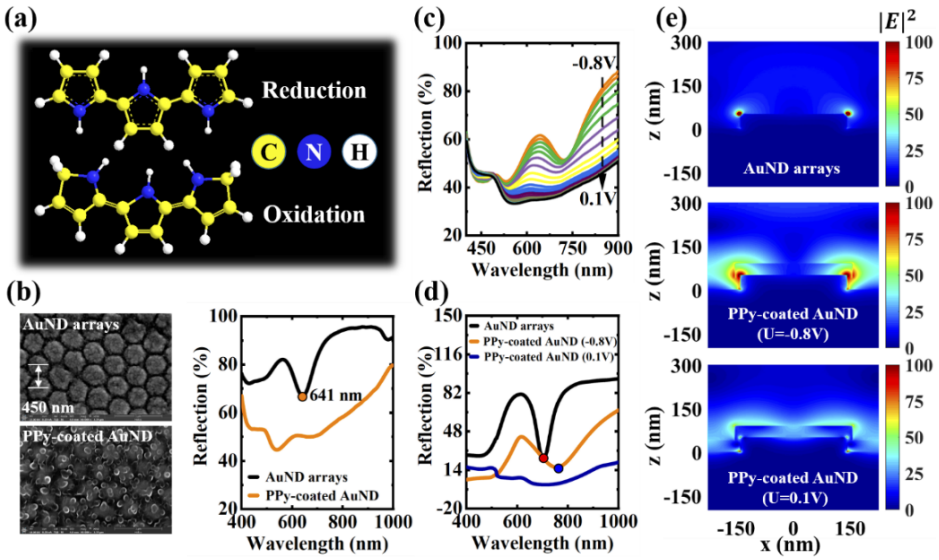

Fig. 2. The electrically controlled optical responses of PPy-coated AuND arrays and the corresponding numerical simulation. (a) The molecular structures of PPy in the reduced and oxidized forms. (b) The measured SEM images and reflection spectra of AuND arrays deposited with and without PPy layer. The orange circle marks the position of the resonant wavelength of bare AuND arrays. (c) The evolution of reflection spectra of PPy-coated AuND arrays for various voltages in the range from −0.8 V to 0.1 V with the step of 0.05 V. (d) The simulated reflection spectra of bare AuND arrays and AuND arrays coated by reduced and oxidized PPy thin layers and (e) their corresponding electric field profiles at the wavelength of 900 nm.

to 0.1 V with a step of 0.05 V, where the structural coloration is obtained by utilizing measured reflection spectra at different voltages in Fig. 2(c). It can be observed clearly that the generated plasmonic color can be fine-tuned from mauve to sky blue under the voltages from −0.8 V to 0.1 V. To further quantitatively investigate the extent and tendency of color variation, the colors in the RGB color space in Fig. 3(a) are transformed into the HSV color space characterized by three main primary elements, hue (H), saturation (S), and value (V) [21]. Figure 3(b) demonstrates the variation of three primary elements at different applied voltages. We observe that, with the increase of the applied voltage, the color hue (H) decreases firstly and it almost remains unchanged after the voltage of −0.2 V. Interestingly, the variation tendency of color saturation (S) is justly opposite to color hue (H). Color value, different from the other elements, is not affected basically by the applied voltages. The change of the above three color elements at different voltages exactly causes the coloration variation of PPy-coated AuND arrays. Furthermore, we investigate its reflection intensity at 900 nm versus time with the two voltages switching from −0.8 V (reduced state) to 0.1 V (oxidized state), as shown in Fig. 3(c). Observably, the reflection intensity at 900 nm is electrically switched from 53% to 88% with the first cycle. Even after 15 cycles within a period of 600 s, the reflection intensity is close to their initial states only with degradation of approximately 2.9%, demonstrating good reversibility and durability for PPy polymer. The slight degradation might be caused by the volume expansion of the PPy layer and irreversible chemical reactions during the electrical modulation. The switching time of PPy-coated AuND arrays is also investigated in Figs. 3(d) and 3(e), where the zoomed view of the first cycle is displayed. We analyze the rise time and the fall time, defined as the time interval in which the current (or intensity) rises and falls between 0% and 95%, respectively. As a result,

Optics EXPRESS

a rise time of 206 ms and the fall time of 218 ms are obtained respectively with the switching of applied voltages, which illustrates that we can obtain the shortest switching time of 424 ms, roughly equivalent to a maximum switching frequency of 2 Hz. This switching time could be further optimized by improving the deposition quality of PPy polymer. It is worth noting that the functionality and practicability of proposed PPy-coated AuND arrays can be expanded by optimizing the design of plasmonic nanostructure.

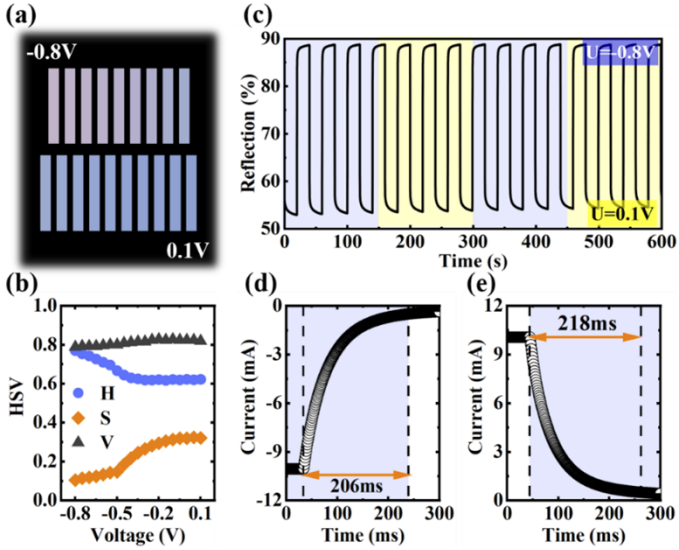

Fig. 3. The electrical switching properties of PPy-coated AuND arrays. (a) The evolution of coloration of PPy-coated AuND arrays under various applied voltages obtained by utilizing the measured reflection spectra at different voltages. (b) The changes of the corresponding hue (H), saturation (S), and value (V) of coloration under various voltages. (c) The reversible modulation of reflected intensity at the wavelength of 900 nm at the two voltages between −0.8 V to 0.1 V. (d) The detailed analysis of the rise time of 206 ms and (e) the fall time of 218 ms for the first switching cycle.

3.2. Electrically switchable responses of PANI-coated AuND arrays

To analyze the distinction of the electrically switchable responses of various conductive polymers-coated AuND arrays, in addition to the PPy polymer, we also investigate the electrical modulation of another conductive EC polymer, PANI, on the optical properties of the AuND arrays, as shown in Fig. 4. Different from the PPy mentioned above with bistable states, PANI has three well-defined states: a fully reduced state (leucoemeraldine), half oxidized state (emeraldine), and full oxidation state (pernigraniline) [22]. The molecular structures of PANI in the fully reduced and oxidized forms are illustrated in Fig. 4(a). In both structures, the electrons of all nitrogen atoms on the structural chain are in a similar state. Any nitrogen atom can attract protons of the dopant, and there may be some protonated nitrogen atoms or free nitrogen atoms binding side by side on the PANI chain, resulting in a low probability of conduction for the polaron. Figure 4(b) demonstrates the reflection spectra of AuND arrays before and after the deposition of a thin PANI layer, depicted by black and orange solid lines, respectively. It can be observed that the conformable covering of the PANI layer causes the plasmonic resonant wavelength of AuND arrays to have a redshift of 28 nm from 659 nm to 687 nm, whilst its resonance reflection intensity also increases. It is noticeable that a remarkable redshift of the resonant wavelength is

Optics EXPRESS

mainly induced by PANI polymer, which is different from the decrease of reflection intensity over a relatively broad spectral range. Therefore, in the electrically modulated response of PANI, we mainly concentrate on the shift of plasmonic resonant wavelength induced by PANI polymer. Figure 4(c) shows the reflection spectra of PANI-coated AuND arrays at the applied voltage from −0.2 V to 0.5 V with a step of 0.1 V. It can be seen clearly that the plasmonic resonance wavelength of PANI-coated AuND arrays has a successive blueshift of 33 nm from 685 nm to 652 nm, which mainly origins from the change of the real part of the refractive index of PANI polymer under different voltages [23]. Remarkably, when the applied voltage sweeps from 0.5 V to 1 V, the resonant wavelength has a reversed shift from 652 nm to 733 nm, as shown in Fig. S2. A redshift up to 81nm is achieved for the plasmon mode, which is much larger than some previously reported literature [24]. The effectively modulated role of PANI polymer makes it a promising candidate for dynamic plasmonic color generation [25]. Similarly, Fig. 4(d) demonstrates the calculated color palettes of PANI-coated AuND arrays at the voltages from −0.2 V to 1 V with a step of 0.1 V. We only observe faint color variations from bright blue to dark blue, which is mainly attributed to the original spectral characteristics of bare AuND arrays. Figure 4(e) shows the variation of three primary elements, hue (H), saturation (S), and value (V) in the HSV color space. During the applied voltages changing from −0.2 V to 1 V, it is observed that the color saturation S has a continuous and relatively large increase compared to the faint change of hue (H) and value (V), which is consistent with the observed result in Fig. 4(d) that the coloration of PANI-coated AuND arrays gradually become darker with the increase of the applied voltages. The electrically modulated stability and switching time of PANI-coated AuND arrays are investigated in Fig. 4(f), where the plasmonic resonance wavelength of PANI-coated AuND arrays can be reversibly switched between 685 nm and 652 nm at the applied voltages of −0.2 V and 0.4 V. There is no degradation observed after15 switching cycles with the time of 600 s. The rise and fall part of the first cycle in Fig. 4(f) is displayed in Fig. 4(g) and 4(h), respectively. We obtain a rise time of 11 ms and a fall time of 45 ms and thus a shortest duty cycle time of 56 ms, which is nearly an order of magnitude less than the counterpart of PPy-coated AuND arrays. Additionally, in our experiment, the cycle stability of our fabricated PANI-coated AuND arrays is poor compared to the PPy polymer because the acidic electrolyte of PANI is easy to cause PANI thin layer to fall off from the AuND arrays.

3.3. *Electrically switchable responses of PEDOT-coated AuND arrays*

In this work, besides the above-mentioned two conductive EC polymers, the third common conductive polymer, PEDOT, is also investigated, as demonstrated in Fig. 5. Different from the PPy and PANI synthesized by the CV method, in our experiment, PEDOT is polymerized on the surface of AuND arrays at a constant voltage of 1.2 V versus Ag/AgCl with its thickness controlled by the polymerization time. The electrochemical oxidation-reduction reaction mechanism of PEDOT is highly similar to the case of PPy polymer. Figure 5(a) depicts the molecular structures of PEDOT in the reduced and oxidized forms. In the process of oxidative doping, the backbone of PEDOT is oxidized to a conductive state accompanied by doping of anions in the electrolyte. In the reduction process, the backbone is reduced to a neutral state accompanied by dedoping of anions. Similar to the other two polymers, Fig. 5(b) demonstrates the reflection spectra of AuND arrays deposited with and without the PEDOT layer. It can be observed that bare AuND arrays exhibit a plasmonic resonance mode at 649 nm marked by a filled orange dot. This plasmonic resonance mode redshifts to 661 nm and has a small change for its whole line shape due to the covering of a nearly fully oxidized PEDOT layer. Obviously, the PDEOT layer only causes weak absorption and a small redshift of plasmonic mode, which is different from PPy and PANI polymers. As shown in Fig. 5(c), applying the voltages from −0.4 V to 0.4 V with a step of 0.1 V, PEDOT-coated AuND arrays have a relatively small increase of the entire reflection intensity and a blueshift of 24 nm from 682 nm to 658 nm for the plasmonic mode. The blueshift of the resonant

Optics EXPRESS

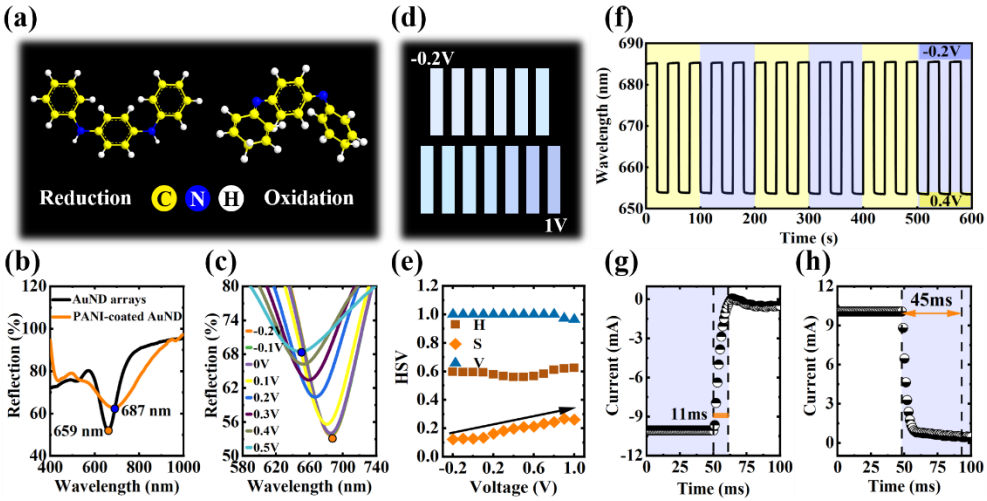

Fig. 4. The electrically switchable properties of PANI-coated AuND arrays. (a) The molecular structures of PANI in the fully reduced and fully oxidized forms. (b) The measured reflection spectra of AuND arrays deposited with and without the thin PANI layer. (c) The evolution of reflection spectra of PANI-coated AuND arrays for various voltages in the range from −0.2 V to 0.5 V with a step of 0.1 V. (d) The color variation of PANI-coated AuND arrays under the voltages from −0.2 V to 1 V. (e) The changes of the corresponding hue (H), saturation (S), and value (V) of coloration under various voltages. (f) The reversibly electric switching of plasmonic resonant wavelength between 685 nm to 652 nm at the applied voltages of −0.2 V to 0.4 V. (g) The detailed analysis of the rise time of 11 ms and (h) fall time of 45 ms for the first cycle.

wavelength and the increase of reflection intensity (equivalent to the decrease of absorption) are attributed to the synchronous decrease of the real part and imaginary part (extinction coefficient) of the refractive index with the growth of applied voltages [26]. Due to the small variation of reflection spectra in Fig. 5(c), the adjusting of coloration is also faint under different voltages (Fig. 5(d)). As shown in Fig. 5(e), a slight change of color of PEDOT-coated AuND arrays is mainly attributed to the degradation of color saturation S, causing the lighter coloration with the increase of applied voltages. The electrical switching of PEDOT-coated AuND arrays is also investigated between the reduced and oxidized states at the applied voltages of −0.4 V and 0.4 V by recording the plasmonic resonant wavelength, as shown in Fig. 5(f). During the first cycle, the resonant wavelength is electrically switched between 682 nm to 658 nm. Unfortunately, there is a slight degradation observed after 15 switching cycles. However, for PEDOT-coated AuND arrays, a fast switching time of 24 ms for a cycle with a rise time of 7 ms and a fall time of 17 ms (Figs. 5(g) and 5(h)) is obtained, which is shorter than the case of PPy and PANI polymer. Therefore, the short switching time of PEDOT in a plasmonic hybrid structure makes it promising for the application of plasmonic video displays with high refresh rates.

3.4. *Comparative analysis and discussion*

An ideal active electrically modulated optical component should have a stable cycle, long lifetime, low energy consumption, and short response time for practical applications. For these three common polymers, the energy consumption during the electrical switching is relatively low, and the corresponding modulation voltage does not exceed 1V. However, there are some differences in the cyclic stability, lifetime, response time, and spectral response between the three polymers,

Optics EXPRESS

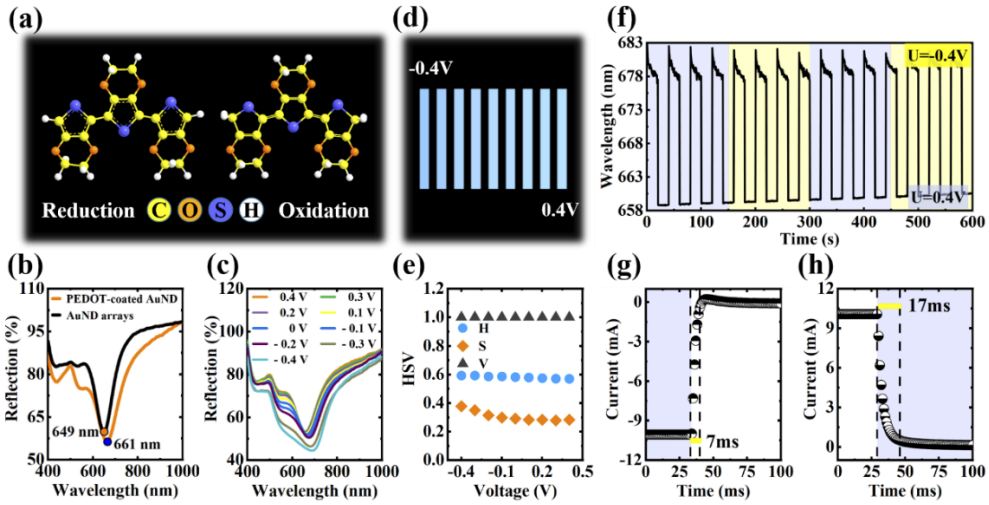

Fig. 5. The electrical switching properties of PEDOT-coated AuND arrays. (a) The molecular structures of PEDOT in the reduced and oxidized forms. (b) The measured reflection spectra of AuND arrays coated with and without the PEDOT layer. (c) The evolution of reflection spectra of PEDOT-coated AuND arrays for the voltages from −0.4 V to 0.4 V with a step of 0.1 V. (d) The color variation of PEDOT-coated AuND arrays under various voltages. (e) The changes of the corresponding hue (H), saturation (S), and value (V) of coloration under various voltages. (f) The electrical switching of resonant wavelength of plasmonic mode in the range from 682 nm to 658 nm during 15 cycles. (g) The detailed analysis of the rise time of 7 ms and (h) fall time of 17 ms for the first cycle.

which are further summarized in Table 1. After 15 cycles, PANI-coated AuND arrays produce almost no degradation, and the other two polymers show slight degradation, especially for the PEDOT polymer. Notably, in our experiment, after more than 15 cycles, the electrical switching capacities of PANI and PEDOT-coated AuND arrays plummeted due to the falling off and the volume expansion of the polymer layer. However, PPy-coated AuND arrays still have a good performance after 50 switching cycles (Supplement 1, Fig. S3), demonstrating excellent switching stability. Additionally, PANI and PEDOT polymers exhibit ultra-fast switching time and refresh rate, particulate for PEDOT with the shortest switching time of less than 25 ms. However, there is no advantage in the switching time of PPy polymer. Furthermore, the PPy polymer is more prone to adjust the bright and dark response of the structure by changing its self-absorption over a broad spectral range due to the simultaneous change of complex dielectric function in both real and imaginary parts. In contrast, the PANI polymer has an advantage over the modulating plasmonic resonance frequency. Therefore, we need to select the most appropriate and optimal polymer to construct high-performance active optoelectronic devices according to their specific functions and practical application scenarios.

In the above results, the switching cycle time of the proposed polymer-coated plasmonic dynamic devices has certain limitations for its practical application. The insufficient cycle stability is primarily attributed to the embrittlement and eventually falling off of the polymer layer induced by the volume expansion of thin polymer film during electrical modulation. Here, some probable strategies are proposed to improve the cyclic stability in future investigations. Firstly, the CV and galvanostatic (GS) combined technique is a possible synthesis method for the polymer film with better electrochromic stability [27]. This is because the small-size polymer nanoparticles obtained by the GS method can be used to fill the space between the large-size

Optics EXPRESS

Table 1. Comparison of electrically switchable properties for three polymer-coated plasmonic hybrid systems

Specification	PPy	PANI	PEDOT
Degradation after 15 switching cycles	≈2.9%	≈0%	≈12.5%
Lifetime	>50 cycles	>15 cycles	>15 cycles
Rise time	206 ms	11 ms	7 ms
Fall time	218 ms	45 ms	17 ms
Shortest switching time	424 ms	56 ms	24 ms
Wavelength/intensity modulation	53% to 88% at 900 nm	685 nm to 733 nm	682 nm to 658 nm

polymer particles obtained by the CV method to form a dense polymer film, efficiently improving the adhesion strength of the polymer. Secondly, inorganic-organic composite materials can be used to improve the cyclic stability of devices, such as poly(5-formylindole) (P5FIn)/WO3 nanocomposites [28] and PANI-fNiO composite [29]. This improvement could be attributed to the ion diffusion channels from the interaction between polymer and inorganic material and the porous surface morphology of nanocomposites, almost avoiding the volume change of the electrode material in doping and dedoping. Thirdly, some new modified conductive polymer monomers also exhibit excellent cycle stability, such as sidechain-modified EDOT derivatives [30] and TAFPy-MA (poly-1,3,6,8-tetramino (furfuryl glycidyl ether)-pyrene-bismaleimide) cross-linking polymer [31]. In this strategy, the excellent operation stability is attributed to the formation processes and further electrochemical polymerization of the polymer chain.

4. Conclusions

In summary, we have demonstrated the electrical modulation of different electrochromism conductive polymers on the optical properties of plasmonic AuND arrays. For these hybrid structures of polymer-coated AuND arrays, the electrical switching response of their reflection spectra and corresponding structural colors have been systematically investigated by applying the voltage to the polymer-coated AuND arrays. Through systematic analysis and comparison, their respective advantages for each conductive polymer are achieved for constructing plasmonic-coated electro-optical active devices. The PPy polymer is preferably available for intensity modulation devices due to its significant changes in absorption at an external voltage and excellent cycle stability. In contrast to the PPy polymer, the PANI polymer is very efficient in modulating the resonance frequency over a broad spectral range, accompanied by a rapid response time of less than 50 ms. However, there is no outstanding advantage for the PEDOT polymer in the modulation of both intensity and resonance frequency. This work provides a valuable technical approach for the selection of conductive polymers to realize high-performance electro-optical active devices for the research community.

5. Materials and methods

Chemical reagent: Aniline, pyrrole (Py), 3,4-ethylenedioxythiophene (EDOT), ethanol, nitric acid (HNO_3), sodium nitrate ($NaNO_3$), sodium perchlorate ($NaClO_4$), acetonitrile, tetrabutylammonium hexafluorophosphate ($TBAPF_6$) and acetone are purchased from Aladdin. A 0.1 M aqueous solution of $NaClO_4$, a 2 M aqueous solution of HNO_3, and a 0.1 M $TBAPF_6$-acetonitrile solution are prepared as the electrolyte solutions of three polymers of PPy, PANI, and PEDOT, respectively. The 200-nm-thick ITO coated glass slides with a size of 5×0.8 cm^2 are successively sonicated in acetone, ethanol, and deionized water for 5 minutes and dried under a stream of nitrogen before being used. The detailed process of preparation of the AAO template has been described in our previous works [17].

Optics EXPRESS

The synthesis of three polymers: PPy is synthesized electrochemically on the surface of AuND arrays with cyclic voltammetry (CV) by scanning the voltage from −0.8 V to 0.7 V versus Ag/AgCl at a rate of 20 mV s^{-1} in an aqueous solution containing 0.1 M $NaClO_4$ and 0.02 M monomer Py. PANI is also synthesized with CV by scanning the voltage from −0.2 V to 1.2 V versus Ag/AgCl at a rate of 30 mV s^{-1} in an aqueous solution involving 2 M HNO_3 and 0.05 M aniline. The thickness of the above two polymers is controlled by the number of CV cycles. PEDOT is synthesized from a 0.1 M $TBAPF_6$-acetonitrile solution containing 0.02 M EDOT at a constant voltage of 1.2 V versus Ag/AgCl. Its film thickness is controlled by synthesized time. All polymer films are rinsed with the monomer-free electrolyte solution. Electrically switchable optical measurements of PPy and PEDOT-coated AuND arrays are carried out in their respective monomer-free electrolyte solutions. A mixed aqueous solution of 0.1 M HNO_3 and 1 M $NaNO_3$ is used for the case of PANI film.

Numerical method: The finite-difference time-domain (FDTD) numerical method is adopted to calculate the reflection spectra and electromagnetic field distributions of PPy-coated AuND arrays. The boundary conditions along the x and y directions are set to periodic conditions, and perfectly matched layers are applied in the z-direction. The mesh size of 2 nm×3.46 nm×1 nm is used in all numerical calculations. The permittivity of Au and Cr are both from Johnson and Christy [32,33], and the refractive index of PPy at the fully reduced states is obtained using an Ellipsometer, as shown in Supplementary Fig. S1. Notably, the refractive index used at oxidized states is two times larger than the case in the fully reduced state.

Funding. National Natural Science Foundation of China (61705100, 61727816, 62171076); Central University Basic Research Fund of China (DUT20RC(3)008).

Acknowledgments. The authors acknowledge the financial support of DUT-BSU international cooperative project. The authors are thankful to Hao He for help in the experiment process and Hongxu Li for help with the paper drawing.

Disclosures. The authors declare no conflicts of interest.

Data availability. Data underlying the results presented in this paper are not publicly available at this time but may be obtained from the authors upon reasonable request.

Supplemental document. See Supplement 1 for supporting content.

References

1. G. K. Shirmanesh, R. Sokhoyan, P. C. Wu, and H. A. Atwater, "Electro-optically Tunable Multifunctional Metasurfaces," ACS Nano **14**(6), 6912–6920 (2020).
2. W. Yang, S. Xiao, Q. Song, Y. Liu, Y. Wu, S. Wang, J. Yu, J. Han, and D.-P. Tsai, "All-dielectric metasurface for high-performance structural color," Nat. Commun. **11**(1), 1864 (2020).
3. T. Xu, E. C. Walter, A. Agrawal, C. Bohn, J. Velmurugan, W. Zhu, H. J. Lezec, and A. A. Talin, "High-contrast and fast electrochromic switching enabled by plasmonics," Nat. Commun. **7**(1), 10479 (2016).
4. A. Ahmadivand, B. Gerislioglu, Z. Ramezani, A. Kaushik, P. Manickam, and S. A. Ghoreishi, "Functionalized terahertz plasmonic metasensors: Femtomolar-level detection of SARS-CoV-2 spike proteins," Biosens. Bioelectron. **177**, 112971 (2021).
5. R. Kaissner, J. Li, W. Lu, X. Li, F. Neubrech, J. Wang, and N. Liu, "Electrochemically controlled metasurfaces with high-contrast switching at visible frequencies," Sci. Adv. **7**(19), eabd9450 (2021).
6. Y. Jin, J. Liang, S. Wu, Y. Zhang, L. Zhou, Q. Wang, H. Liu, and J. Zhu, "Electrical Dynamic Switching of Magnetic Plasmon Resonance Based on Selective Lithium Deposition," Adv. Mater. **32**(42), 2000058 (2020).
7. M. N. Yao, T. F. Li, Y. B. Long, P. Shen, G. X. Wang, C. L. Li, J. S. Liu, W. B. Guo, Y. F. Wang, L. Shen, and X. W. Zhan, "Color and transparency-switchable semitransparent polymer solar cells towards smart windows," Sci. Bull. **65**(3), 217–224 (2020).
8. K. R. Reyes-Gil, Z. D. Stephens, V. Stavila, and D. B. Robinson, "Composite WO3/TiO2 Nanostructures for High Electrochromic Activity," ACS Appl. Mater. Interfaces **7**(4), 2202–2213 (2015).
9. X. Y. Duan and N. Liu, "Magnesium for Dynamic Nanoplasmonics," Acc. Chem. Res. **52**(7), 1979–1989 (2019).
10. M. Zhang and Z. Y. Song, "Switchable terahertz metamaterial absorber with broadband absorption and multiband absorption," Opt. Express **29**(14), 21551–21561 (2021).
11. D. Franklin, R. Frank, S.-T. Wu, and D. Chanda, "Actively addressed single pixel full-colour plasmonic display," Nat. Commun. **8**(1), 15209 (2017).
12. H. Zhang, S. L. Ming, Y. Z. Liang, L. Feng, and T. Xu, "A Multi-color Electrochromic Material based on Organic Polymer," Int. J. Electrochem. Sci. **15**(2), 1044–1057 (2020).

Optics EXPRESS

13. L. Shao, X. Zhuo, and J. Wang, "Advanced Plasmonic Materials for Dynamic Color Display," Adv. Mater. **30**(16), 1704338 (2018).
14. Y. Shi, L. J. Pan, B. R. Liu, Y. Q. Wang, Y. Cui, Z. A. Bao, and G. H. Yu, "Nanostructured conductive polypyrrole hydrogels as high-performance, flexible supercapacitor electrodes," J. Mater. Chem. A **2**(17), 6086–6091 (2014).
15. T. Wang, Y. Zhang, Q. Liu, W. Cheng, X. Wang, L. Pan, B. Xu, and H. Xu, "A Self-Healable, Highly Stretchable, and Solution Processable Conductive Polymer Composite for Ultrasensitive Strain and Pressure Sensing," Adv. Funct. Mater. **28**(7), 1705551 (2018).
16. K. Xiong, D. Tordera, G. Emilsson, O. Olsson, U. Linderhed, M. P. Jonsson, and A. B. Dahlin, "Switchable Plasmonic Metasurfaces with High Chromaticity Containing Only Abundant Metals," Nano Lett. **17**(11), 7033–7039 (2017).
17. Y. Liang, W. Cui, L. Li, Z. Yu, W. Peng, and T. Xu, "Large-Scale Plasmonic Nanodisk Structures for a High Sensitivity Biosensing Platform Fabricated by Transfer Nanoprinting," Adv. Opt. Mater. **7**(7), 1801269 (2019).
18. Y. Huang, H. F. Li, Z. F. Wang, M. S. Zhu, Z. X. Pei, Q. Xue, Y. Huang, and C. Y. Zhi, "Nanostructured Polypyrrole as a flexible electrode material of supercapacitor," Nano Energy **22**, 422–438 (2016).
19. R. Celiesiute, A. Ramanaviciene, M. Gicevicius, and A. Ramanavicius, "Electrochromic Sensors Based on Conducting Polymers, Metal Oxides, and Coordination Complexes," Crit Rev Anal Chem **49**(3), 195–208 (2019).
20. J. C. Gustafsson, O. Inganas, and A. M. Andersson, "CONDUCTIVE POLYHETEROCYCLES AS ELECTRODE MATERIALS IN SOLID-STATE ELECTROCHROMIC DEVICES," Synth. Met. **62**(1), 17–21 (1994).
21. G. Paschos, "Perceptually uniform color spaces for color texture analysis: An empirical evaluation," IEEE Trans. on Image Process. **10**(6), 932–937 (2001).
22. M. Shahabuddin, T. McDowell, C. E. Bonner, and N. Noginova, "Enhancement of Electrochromic Polymer Switching in Plasmonic Nanostructured Environment," ACS Appl. Nano Mater. **2**(3), 1713–1719 (2019).
23. R. Greef, M. Kalaji, and L. M. Peter, "Ellipsometric studies of polyaniline growth and redox cycling," Faraday Discuss. Chem. Soc. **88**, 277–289 (1989).
24. S. Zhang, L. Feng, H. Zhang, M. Z. Liu, and T. Xu, "Electrochromic modulation of plasmonic resonance in a PEDOT-coated nanodisk metasurface," Opt. Mater. Express **10**(4), 1053–1060 (2020).
25. Y. R. Leroux, J. C. Lacroix, K. I. Chane-Ching, C. Fave, N. Felidj, G. Levi, J. Aubard, J. R. Krenn, and A. Hohenau, "Conducting polymer electrochemical switching as an easy means for designing active plasmonic devices," J. Am. Chem. Soc. **127**(46), 16022–16023 (2005).
26. A. Baba, J. Lubben, K. Tamada, and W. Knoll, "Optical properties of ultrathin poly(3,4-ethylenedioxythiophene) films at several doping levels studied by in situ electrochemical surface plasmon resonance spectroscopy," Langmuir **19**(21), 9058–9064 (2003).
27. K. Zhou, H. Wang, J. Jiu, J. Liu, H. Yan, and K. Suganuma, "Polyaniline films with modified nanostructure for bifunctional flexible multicolor electrochromic and supercapacitor applications," Chem. Eng. J. **345**, 290–299 (2018).
28. Q. Guo, X. Zhao, Z. Li, D. Wang, and G. Nie, "A novel solid-state electrochromic supercapacitor with high energy storage capacity and cycle stability based on poly(5-formylindole)/WO3 honeycombed porous nanocomposites," Chem. Eng. J. **384**, 123370 (2020).
29. M. Jamdegni and A. Kaur, "Highly efficient dark to transparent electrochromic electrode with charge storing ability based on polyaniline and functionalized nickel oxide composite linked through a binding agent," Electrochim. Acta **331**, 135359 (2020).
30. S. Macher, M. Schott, M. Sassi, I. Facchinetti, R. Ruffo, G. Patriarca, L. Beverina, U. Posset, G. A. Giffin, and P. Löbmann, "New Roll-to-Roll Processable PEDOT-Based Polymer with Colorless Bleached State for Flexible Electrochromic Devices," Adv. Funct. Mater. **30**(6), 1906254 (2020).
31. R. Zheng, Y. Wang, J. Pan, H. A. Malik, H. Zhang, C. Jia, X. Weng, J. Xie, and L. Deng, "Toward Easy-to-Assemble, Large-Area Smart Windows: All-in-One Cross-Linked Electrochromic Material and Device," ACS Appl. Mater. Interfaces **12**(24), 27526–27536 (2020).
32. P. B. Johnson and R. W. Christy, "OPTICAL CONSTANTS OF NOBLE METALS," Phys. Rev. B **6**(12), 4370–4379 (1972).
33. P. B. Johnson and R. W. Christy, "Optical constants of transition metals: Ti, V, Cr, Mn, Fe, Co, Ni, and Pd," Phys. Rev. B **9**(12), 5056–5070 (1974).